Poly(methyl Methacrylate) Membranes

YOSHITADA SAKAI and HIROSHI TANZAWA, *Basic Research Laboratory Toray Industries, Inc., Kamakura, Kanagawa, Japan*

Synopsis

Uniform and symmetric membranes were formed from poly(methyl methacrylate) (PMMA) by making use of the stereocomplex phenomenon which characteristically occurs in the solution of a mixture of isotactic PMMA and syndiotactic PMMA. The water permeability of the membrane was very high compared to a commercially available cellulosic membrane, whereas their NaCl permeabilities were the same. The permeabilities of the membranes are explained by a simple capillary model. By varying the tacticity of the polymer it was found that the finest membrane structure is formed at the isotactic polymer ratio of ca. 30%. This shows the close relationship between complex formation and membrane permeability.

INTRODUCTION

To attain a usable membrane of appropriate permeability and proper mechanical properties, it is generally imparative to produce gelation, which fixes the physical structure in a way which is similar to that of the polymer in solution. In the gelation process for maintaining membrane structure, various mechanisms are utilized according to the kind of polymer, as shown in Table I.

With the hydrophilic polymers, for example, poly(vinyl alcohol) (PVA),[1,2] poly(N-vinylpyrrolidone) (PVP),[3] poly(acryl amide) (PAAm),[4] and poly(hydroxyethyl methacrylate) (PHEMA),[5] membrane structures swollen by water are maintained by the introduction of covalent bonding at the same time as, or after, polymerization. With polyion complex membranes (PIC), ionic bonding between the cationic and anionic polymers is used for maintaining membrane structure.[6] With cellulose acetate membranes (CA), which are most typically used as reverse osmosis membranes, and for cellulose membranes (C), which are used as dialysis membranes, microcrystals formed by hydrogen bonding contribute to maintaining the membrane structure.[7,8]

Apart from these cases, nobody has succeeded in preparing water-swollen membranes solely from poly(methyl methacrylate) (PMMA)[9] because of the hydrophobicity of the material. When PMMA is dissolved in a solvent miscible with water, such as dimethyl sulfoxide (DMSO), and the solution is immersed into water, precipitate formation occurs, as common PMMA polymerized radically is atactic and noncrystalizable. Of course, introducing chemical crosslinking

TABLE I
Mechanisms for Maintaining Membrane Structure for Various Polymers

Bonding	Examples
Covalent	PVA, PVP, PAAm, PHEMA
Ionic	PIC
Hydrogen	CA, C
Hydrophobic	PMMA

Journal of Applied Polymer Science, Vol. 22, 1805–1815 (1978)

0021-8995/78/0022-1805$01.00

into PMMA is completely useless, because it does not have swelling activity in water.

On the other hand, it is well known that there occurs a complex formation between isotactic PMMA and syndiotactic PMMA. This stereocomplex phenomenon, which is a thermoreversible sol–gel phase transition phenomenon, was found at first as a gelation phenomenon of the dimethylformamide solution of PMMA.[10] Since then, similar solution systems have been examined by many methods such as viscometry, light scattering, infrared spectrometry, ultraviolet spectrometry, x-ray diffractometry, nuclear magnetic resonance spectrometry, ultracentrifugation, thin-layer chromatography, and thermal analysis.[11–14] As a result of these analyses, this phenomenon has been attributed to stoichiometric and thermoreversible crosslinking by the hydrophobic bonding between the isotactic and syndiotactic parts of polymers.

This phenomenon was used for preparing our membranes. It was found that the PMMA membranes have some characteristic permeabilities which seem to be derived from the hydrophobicity of the material and which are not found in hydrophilic membranes, and so are interesting from a practical point of view. Symmetric and uniform membranes which have various membrane structures can be made. These membranes are also interesting as model membranes for basic research on membrane permeation phenomena.

EXPERIMENTAL

Membrane Preparation

The basic processes of membrane preparation are shown in Figure 1. Polymers polymerized anionically were used as isotactic elements of PMMA (Iso). The isotacticity of these polymers calculated from the triad spectrum of NMR[15] was more than 95%. Polymers polymerized radically were used as syndiotactic elements of PMMA (Syn). The tacticity of these polymers was: syndiotacticity 55%, heterotacticity 32%, isotacticity 13%; therefore these polymers are more appropriately called atactic polymers rather than syndiotactic polymers. The molecular weight of the polymers was in the range of 1.3×10^5 to 1.45×10^6. As membranes were prepared under quasi-equilibrated conditions, it was found that the molecular weight of the polymers does not affect permeabilities.

DMSO was used as solvent. The polymer concentration in solution was varied between 10 and 40 wt-%. The mixing ratio of both polymers was also varied. The mixture of Iso, Syn, and DMSO was heated and stirred for more than 2 hr above the gelation temperature of the solution. The gelation temperature was

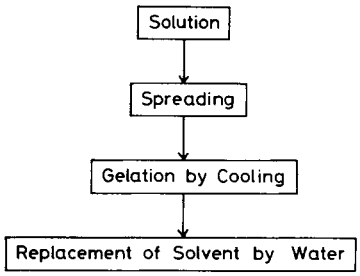

Fig. 1. Basic processes of PMMA membrane preparation.

between about 30° and 95°C, according to the polymer concentration and polymer characteristics such as molecular weight and tacticity.

The solution was held between preheated glass plates in the spreading process. When the sandwiched solution was cooled, it changed to a gel which had enough strength to be held by hand. The gel was immersed into cold water containing ice, and DMSO was replaced by water.

The membranes prepared by this method are generally transparent, and so it is understood that the membrane is of a structure finer than the wavelength of visible light. These membranes are presumably uniform and symmetric as was shown by transmission electron microscopy (see Fig. 2).

Measurement of Permeabilities

The water permeability coefficient L_p is defined by

$$J_v = L_p \, \Delta P \tag{1}$$

where J_v and ΔP are volume flux of water [$cm^3/(cm^2\ sec)$] and pressure difference (dyn/cm^2) across the membrane, respectively. L_p was measured by using a batch filtering cell (membrane area 12 cm^2) and at a water head of 1 meter as ΔP.

The solute permeability coefficient P_2 is defined by

$$J_s = P_2 \frac{\Delta C}{\lambda} \tag{2}$$

where J_s, ΔC, and λ are solute flux [$mole/(cm^2\ sec)$], concentration difference ($mole/cm^3$) across the membrane, and membrane thickness, respectively. P_2 was measured by using a batch dialyzer shown schematically in Figure 3.

The measuring operations for P_2 were as follows: The solution and pure water were put into the concentrate compartment and the diluent compartment, respectively. Both compartments were stirred sufficiently for 30 min to 3 hr, according to the permeability of the membrane. At the end of measuring, the diluent was sampled and analyzed. The coefficient P_2 was calculated by eq. (3), which is the integrated form of eq. (2):

$$P_2 = \frac{2.303\lambda V''}{\left(1 + \frac{V''}{V'}\right) At} \log_{10} \frac{C_0}{C_0 - \left(1 + \frac{V''}{V'}\right) C_t''} \tag{3}$$

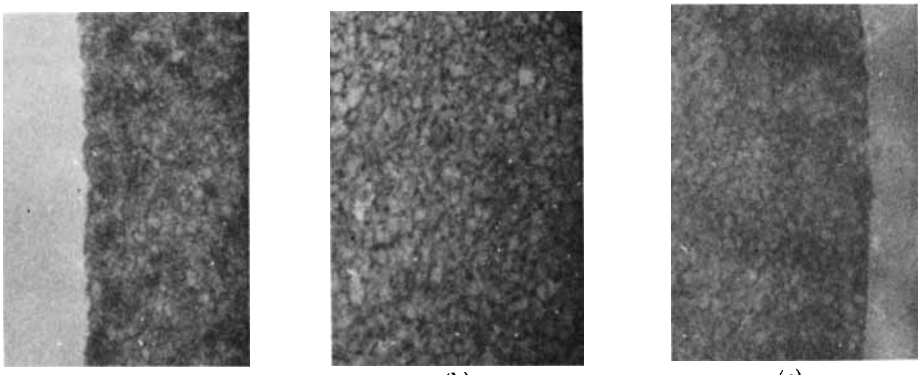

(a) (b) (c)

Fig. 2. Transmission electron micrographs of a PMMA membrane (30,000×): (a) and (c) structure near both surfaces; (b) internal structure.

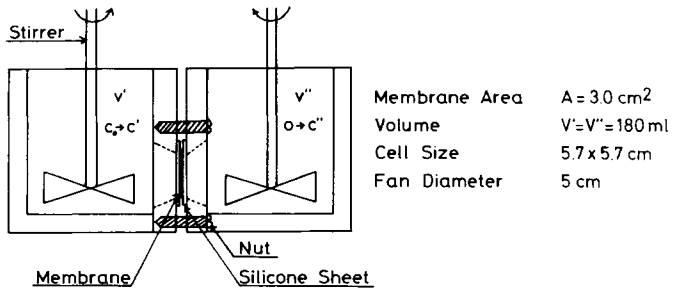

Fig. 3. Batch dialyzer for measuring solute permeability.

where V', V'', A, C_0, and C_t are the volumes of the concentrate and the diluent compartment, effective membrane area, initial concentration of the concentrate, and concentration of the diluent at sampling time t, respectively. The rate of stirring was investigated beforehand by changing the revolution rate, and it was decided upon to be more than 900 rpm, where the boundary resistance is regarded practically as zero.

NaCl and urea were used as solutes. NaCl was analyzed by electric conductometry, and urea was analyzed by spectrometry using p-dimethylaminobenzaldehyde as colorent. Measurements of L_p and P_2 were done at 30° ± 1°C by placing the cells in an air oven.

RESULTS

The dependence of the water content of the membrane, H_w (wet membrane base) on the polymer concentration of the solution is shown in Figure 4, where the ratio of Syn/Iso was fixed at 5/1. It is clear from this figure that the water content greatly depends on polymer concentration, which suggests that the membrane structure reflects the gel structure originating in the stereocomplex phenomenon. In this figure the estimated water content is also shown. This was obtained under the assumption that the pore space of the gel filled with

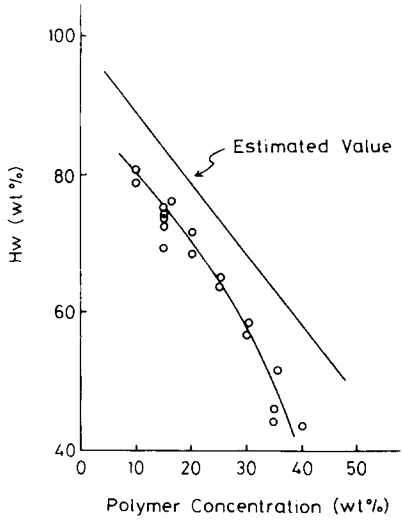

Fig. 4. Dependence of water content on polymer concentration: Syn/Iso = 5/1.

DMSO (density 1.10 g/cm^3) at first is merely refilled with water (density 1.00 g/cm^3). The experimental values are lower than the estimated value by about 10%. This may be attributed to syneresis during the gelation process and a little shrinking during the replacement of DMSO by water.

Figure 5 shows the dependence on water content of water permeability λL_p and NaCl permeability P_2 (NaCl) for the same membranes as those in Figure 4. λL_p and P_2 express the intrinsic water permeability and the intrinsic solute permeability, respectively, normalized by the membrane thickness, as both J_v and J_s are reciprocal to λ in the case of uniform membranes. The degree of dependence of water permeability on water content is very large, but that of solute permeability is small. The values of H_w, λL_p, and P_2 (NaCl) for Cuprophan, a commercially available cellulosic membrane, are 42%, 6.7×10^{-14} g^{-1} cm^3 sec, and 1.7×10^{-6} cm^2 sec^{-1}, respectively. The values of λL_p and P_2 (NaCl) for a PMMA membrane of the same water content as Cuprophan are 1.5×10^{-12} g^{-1} cm^3 sec and 1.8×10^{-6} cm^2 sec^{-1}, respectively. The water permeability of the PMMA membrane is extremely high compared to that of Cuprophan, whereas their solute permeabilities are almost the same. This characteristic is taken as the effect of the hydrophobicity of the membrane material.

In Table II, the ratios of urea permeability P_2 (urea) to NaCl permeability P_2 (NaCl) for various water contents of PMMA membranes are shown. The ratios are constant throughout a very wide range of water content, and the ratios are almost the same as D (urea)/D (NaCl), where D is the diffusion coefficient. This

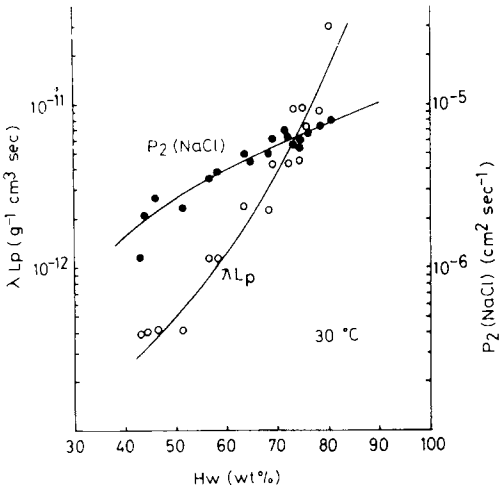

Fig. 5. Dependence of water permeability and NaCl permeability on water content: Syn/Iso = 5/1.

TABLE II
Ratios of Urea Permeability to NaCl Permeability

Hw, wt-%	P_2 (urea)/P_2 (NaCl)
43	1.0
57	1.0
68	1.1
74	0.9
D (urea)/D (NaCl)	0.86

results from the fact that there are no characteristic interactions between the membrane material and the solutes because of the chemical simplicity of the membrane material. It is well known that contrary to PMMA membranes, in the case of reverse osmosis membranes made of cellulose acetate there is a marked difference in the rejection characteristics for urea and NaCl.

In Figure 6 the dependence of water permeability λL_p and NaCl permeability P_2 (NaCl) on the ratio of Iso is shown. For these membranes the polymer concentration of the membrane preparation solution was fixed at 20 wt-%, and the water content of these membranes was practically the same, around 65 wt-%. This figure shows that the water permeability reaches a minimum value at about 30% and that the solute permeability remains almost constant throughout the range of the experiments. Figures 5 and 6 shows that a membrane of a certain water permeability and solute permeability can be designed according to the membrane's intended use. This should have interesting practical implications.

DISCUSSION

It is interesting that membranes of the same material and the same water content have different permeabilities, as shown in Figure 6. Not only this but also the result shown in Figure 5 can be explained using a simple membrane structure model. An interesting understanding of the mechanism of PMMA membrane formation was also obtained. In this capillary model, membrane pores are visualized as straight capillaries perpendicular to the membrane surface, having uniform radii throughout the membrane, as shown in Figure 7. The real membrane structure shown in Figure 2 is quite different from that shown in Figure 7. Nevertheless this simplified model is useful for understanding the permeation characteristics of PMMA membranes.

Water and solutes are thought to penetrate only through these capillaries, according to Hagen-Poiseuille's law and Fick's law, respectively. The solute concentration at the capillary ends is assumed to be the same as the concentration in the outer solution in immediate contact with the capillary; that is, the partition

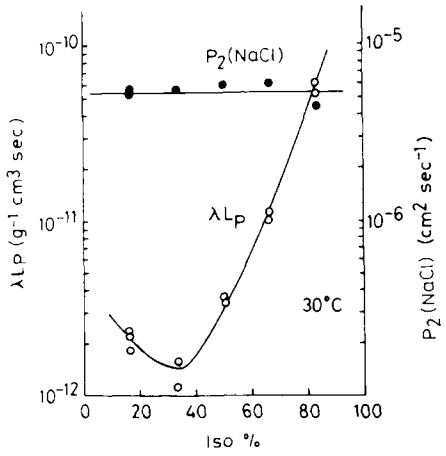

Fig. 6. Dependence of water permeability and NaCl permeability on isotactic polymer ratio: polymer concentration = 20 wt-%.

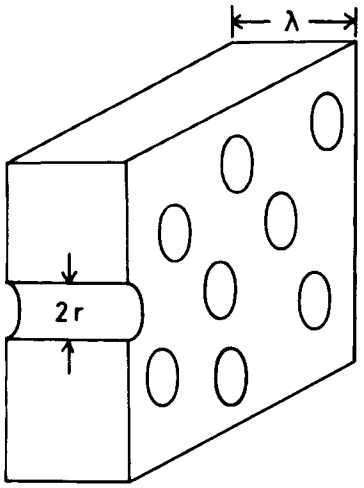

Fig. 7. Capillary model for membrane structure.

coefficient of the solute is assumed to be the same as the water content. According to this model, volumetric water content H, water permeability λL_p, solute permeability P_2, and selectivity $P_2/\lambda L_p$ are expressed as follows:

$$H = \pi n r^2 \tag{4}$$

$$\lambda L_p = \pi n r^4 / 8\eta \tag{5}$$

$$P_2 = \pi n r^2 D = HD \tag{6}$$

$$P_2/\lambda L_p = 8\eta D / r^2 \tag{7}$$

where n, r, η, and D express the capillary number density per unit area, the radius of capillary, the viscosity of water, and the diffusion coefficient of the solute in water, respectively. The ratio $P_2/\lambda L_p$ was designated as the selectivity, because this expression is the ratio between two permeabilities for different substances. This ratio corresponds to the second term $\omega V_s/L_p$ of the expression for the selectivity coefficient σ using resistant coefficients which Katchalski et al. presented.[16] According to these equations, P_2 is the same for membranes of the same water content, whereas λL_p can be different. This characteristic of the model corresponds to the result shown in Figure 6.

In these formulations, all characteristics of the membrane structure are reduced to n and r. They are calculated from measured H and L_p, according to eqs. (8) and (9), which are derived from eqs. (4) and (5):

$$n = \frac{H^2}{8\pi\eta\lambda L_p} \tag{8}$$

$$r = \left(\frac{8\eta\lambda L_p}{H}\right)^{1/2} \tag{9}$$

The dependence of n and r on water content derived from the data in Figure 5 is shown in Figure 8, and the dependence of n and r on the ratio of Iso derived from the data in Figure 6 is shown in Figure 9. The viscosity of water used to calculate these values was 0.800 cP (30°C). As water content, the water content by weight was used, which is considered the same as water content by volume

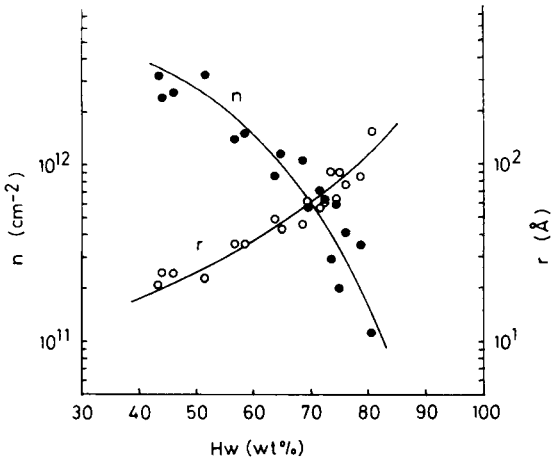

Fig. 8. Dependence of capillary number density and capillary radius on water content: Syn/Iso = 5/1.

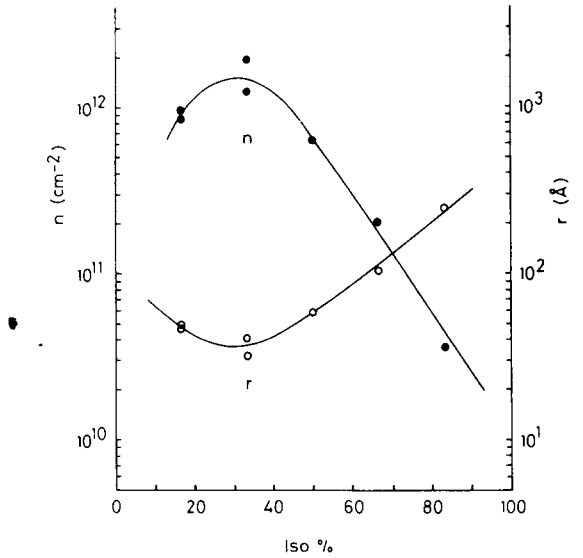

Fig. 9. Dependence of capillary number density and capillary radius on isotactic polymer ratio: polymer concentration = 20 wt-%.

in the case of the water-swollen membrane whose density is approximately 1.0 g/cm^3.

In order to verify if the use of such a simplified model is valid in understanding membrane permeabilities, it is appropriate to use eq. (7), which shows that $P_2/\lambda L_p$ depends only on r, not on n. The dependence of the selectivity $P_2/\lambda L_p$ on r is shown in Figure 10, where the experimental values and the theoretical value expressed by eq. (7) are shown. Both cases shown in Figures 5 and 6 are presented as the experimental values. They are plotted on the same line, showing that both cases in Figures 5 and 6, where they seem to require explanation inasmuch as they differ from each other, can both be understood by the simple model. The slopes of the line for the model and the experiments are 2.0 and 1.7, respectively, so they qualitatively coincide with each other. It is con-

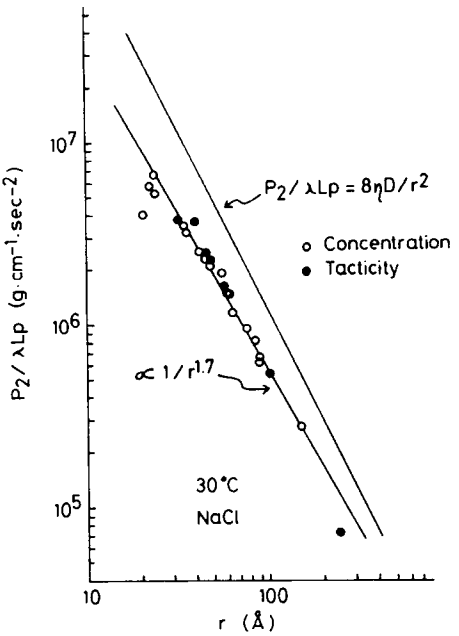

Fig. 10. Dependence of selectivity on capillary radius.

cluded that the model is appropriate, even if not completely, for expressing the permeabilities of the PMMA membranes.

The discrepancy between the values of the model and the experiments shown in Figure 10 derives from the fact that the model for the membrane structure is so simple. The points that are not considered in Figure 7 and that should be considered in a more detailed model are the distribution of pore size and the tortuosity of the pore.

If we assume a distribution function $f(r)$ for pore radius, eqs. (9) and (7) are expressed as follows:

$$r_c = \left(\frac{\int_0^\infty f(r)\, r^4\, dr}{\int_0^\infty f(r)\, r^2\, dr} \right)^{1/2} \tag{10}$$

$$\left(\frac{P_2}{\lambda L_p} \right)_d = 8\eta D \frac{\int_0^\infty f(r)\, r^2\, dr}{\int_0^\infty f(r)\, r^4\, dr} = \frac{8\eta D}{r_c^2} \tag{11}$$

where the suffix c expresses the value calculated from experimental values of H and λL_p and the suffix d expresses the value in the case where the distribution exists.

Equation (11) shows that the relationship between $P_2/\lambda L_p$ and r_c does not change from their relationship expressed by eq. (7) even when a distribution of pore radii exists. So the discrepancy between the model and the experiments does not disappear at all.

The influence of the tortuosity of the pore on the permeability is as follows.

The model for membrane structure shown in Figure 7 is changed to the model where the membrane has capillaries of radius r_t, length λ_t, and number density n_t. In this model, the tortuosity ϵ is defined as follows:

$$\frac{\lambda_t}{\lambda} = \epsilon \tag{12}$$

According to this model, eqs. (9) and (7) are restated as follows:

$$r_c = r_t/\epsilon \tag{13}$$

$$\left(\frac{P_2}{\lambda L_p}\right)_t = \frac{8\eta D}{r_t^2} \tag{14}$$

where the suffix t expresses the values in the case where tortuosity exists. From eq. (13) it is found that r_c calculated from the experimental values of H and λL_p is smaller than r_t, since ϵ is larger than 1. If the expression for the abscissa in Figure 10 is changed from r_c to r_t, the experimental values will shift to the right, whereas the model value expressed by eq. (14) will not move from the line shown in Figure 10. Then the discrepancy between the model and the experiments will disappear. In order to make both values coincide, one only needs to estimate ϵ to be about 1.5. This tortuosity is small compared to the tortuosity commonly considered. Thus it can be concluded that the introduction of a slight tortuosity to the membrane capillary model explains the permeabilities of PMMA membranes.

On the basis of the membrane model, the relationship between the membrane preparation mechanism and its permeability can be further discussed. Figure 8 shows that as the water content increases, the number density of the capillary decreases and at the same time the radius of the capillary increases. That is, a membrane of high water content has a coarse membrane structure.

Figure 9 shows that at a ratio of Iso of about 30%, the number density reaches a maximum and the capillary radius a minimum. That is, the finest membrane structure is found at this polymer ratio. This polymer ratio corresponds to the ratio where the strongest PMMA complex gel forms, which is mentioned in many works discussing the stereocomplex phenomenon as stoichiometric.[11–13] According to these studies, at a polymer ratio of Syn/Iso = 2/1 the strongest complex is formed; and in the membrane preparation this strongest complex contributes to the formation of the finest membrane structure. It is concluded that at this tacticity the density of crosslinking reaches the highest level. This result is slightly different from the belief of Liu et al.[12] that when the strongest complex is formed the crosslinking length between Syn and Iso is longest.

CONCLUSIONS

Membranes were formed from PMMA, which is a purely hydrophobic material, by making use of the stereocomplex phenomenon. As one characteristic, it was found that the water permeability of this membrane is very high compared to a commercially available cellulosic membrane, whereas their NaCl permeabilities are the same. The permeabilities of this membrane are explained by a capillary model allowing for slight tortuosity. When the tacticity of polymer was varied, it was found that at the polymer ratio where the strongest complex is apparently formed, the finest membrane structure is obtained. This shows the close relationship between complex formation and membrane permeability.

The authors wish to thank Dr. M. Itoga for his advice, Mr. K. Yoshimura for the electron microscopy study, and Miss E. Onohara for her assistance.

References

1. M. Odian and E. F. Leonard, *Trans. Am. Soc. Artif. Int. Organs,* **14,** 19 (1968).
2. O. M. Ebra-Lima and D. R. Paul, *J. Appl. Polym. Sci.,* **19,** 1381 (1975).
3. M. Luttinger and C. W. Cooper, *J. Biomed. Mat. Res.,* **1,** 67 (1967).
4. B. D. Halpern, H. Cheng, S. Kno, and H. Greenberg, *Proc. Artificial Heart Program Conference,* Washington, D.C., 1969, p. 87.
5. J. Vacík and J. Kopeček, *J. Appl. Polym. Sci.,* **19,** 3029 (1975).
6. M. K. Vogel, R. A. Cross, H. J. Bixler, and R. J. Guzman, *J. Macromol. Sci. Chem.,* **A4,** 675 (1970).
7. R. E. Kesting, M. K. Barsh, and A. L. Vincent, *J. Appl. Polym. Sci.,* **9,** 1873 (1965).
8. A. M. Staké, F. C. Bock, A. Endres, and T. H. Meltzer, *Appl. Polym. Symp.,* **13,** 285 (1970).
9. H. Yasuda, C. E. Lamaze, and L. D. Ikenberry, *Macromol. Chem.,* **118,** 19 (1968).
10. W. H. Watanabe, C. F. Ryan, P. C. Fleischer, Jr., and B. S. Garrett, *J. Phys. Chem.,* **65,** 896 (1961).
11. A. M. Liquori, G. Anzuino, V. M. Coiro, M. D'Alagni, P. De Santis, and M. Savino, *Nature,* **206,** 358 (1965).
12. H. Z. Liu and K. J. Liu, *Macromolecules,* **1,** 157 (1968).
13. T. Miyamoto and H. Inagaki, *Polym. J.,* **1,** 46 (1970).
14. J. Broš, Z. Máša, and J. Pouchlý, *Eur. Polym. J.,* **10,** 629 (1974).
15. F. A. Bovey and G. V. D. Tiers, *J. Polym. Sci.,* **44,** 173 (1960).
16. O. Kedem and A. Katchalski, *J. Gen. Physiol.,* **45,** 143 (1961).

Received February 14, 1977
Revised April 14, 1977